

MCR-71-80

N71-23666

~~NASA CR-1036~~

NASA CR-103101

Contract NAS8-25054

LONGITUDINAL PROPULSION COUPLING SYSTEM

FINAL REPORT

Volume I - Derivation of Equations of Motion

March 1971

**CASE FILE
COPY**

Prepared for:

George C. Marshall Space Flight Center
Marshall Space Flight Center, Alabama 35812

Prepared by:

Martin Marietta Corporation
Denver Division
Denver, Colorado 80201

Contract NAS8-25054

LONGITUDINAL PROPULSION COUPLING SYSTEM

FINAL REPORT

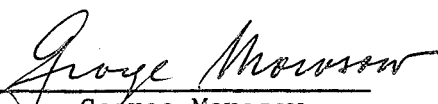
Volume I -- Derivation of Equations of Motion

March 1971

Author

Ronald W. Johnson

Approved


George Morosow
Program Manager

Prepared for:

George C. Marshall Space Flight Center
Marshall Space Flight Center, Alabama 35812

Prepared by:

Martin Marietta Corporation
Denver Division
Denver, Colorado 80201

FOREWORD

The two volumes comprising this report were prepared in the Dynamics and Loads Section, Martin Marietta Corporation, Denver Division, Denver, Colorado, under Contract NAS8-25054. Mr. George Morosow, head of the Dynamics and Loads Section, was Program Manager for this project. Principal Investigator was Ronald W. Johnson.

Mr. Larry Kiefling and Mr. Robert Ryan of NASA's Aero-Astronautics Laboratory, MSFC, Huntsville, served as contract monitors for this program. Several members of Martin's Dynamics and Loads Section made contributions to this effort. These include R. Mathews, R. Philippus, B. Bejmuk, and F. Day.

TABLE OF CONTENTS

	<u>Page</u>
Foreword	ii
Table of Contents	iii
List of Figures	iv
List of Tables	iv
Nomenclature	v
1.0 Introduction	1
2.0 Summary	2
3.0 Derivation of Equations	4
3.1 Introduction	4
3.2 Structure	5
3.3 Lateral Control System	12
3.4 Propellant Feedlines	14
3.5 Pump Cavitation	25
3.6 Propulsion System	31
4.0 Summary of Equations	41
5.0 References	50

LIST OF FIGURES

<u>Figure</u>	<u>Title</u>	<u>Page</u>
3.4.1	Accumulator Representation	24
3.5.1	Pump Schematic	26
3.5.2	Vapor Pressure Curve of the Propellant	27
3.6.1	Typical Propulsion System Schematic	32
3.6.2	Typical Propulsion Discharge Line System	40

LIST OF TABLES

<u>Table</u>	<u>Title</u>	<u>Page</u>
3.1.1	Nomenclature for Structural Matrix Equations	7

NOMENCLATURE

SYMBOL	DEFINITION	UNITS
A_d	Duct area	in^2
A_e	Combustion chamber equivalent exit area	in^2
A_o	Cavitation polytropic flexibility factor	$\text{in}^3 (\text{lb}/\text{in}^2)^{1/n}$
A_s	Duct area at pump inlet	in^2
A_{TB}	Duct area at tank bottom	in^2
A_T	Thrust comb. chamber nozzle throat area	in^2
A_{TG}	Gas generator throat equivalent area	in^2
a_o	Pitch attitude coefficient	-
a_1	Pitch attitude rate coefficient	sec
B	Feedline duct friction factor coefficient	1/sec
C^*	Thrust chamber characteristic velocity	in/sec
C_g^*	Gas generator characteristic velocity	in/sec
C_F	Thrust coefficient	-
C_f	Duct friction loss coefficient per unit length	1/in
C_p	Specific heat of gas generator exhaust products	btu/lb-°R
D_o	Outer diameter of feedline duct wall	in
D_i	Inner diameter of feedline duct wall	in
E	Modulus of elasticity of duct material	lb/in^2
F_P	Force acting at pump, due to feedline pressure	lb
F_{TB}	Force acting at tank bottom, due to feedline pressure	lb

NOMENCLATURE

SYMBOL	DEFINITION	UNITS
\overline{F}_d	Friction and inertial forces acting on fluid feed- line duct	lb/in ² lb/in ²
$F(\dot{\phi})$	Pitch attitude error filter	-
$F(\ddot{\phi})$	Pitch attitude rate error filter	-
g	Acceleration due to gravity	in/sec ²
$^o H$	Total enthalpy	BTU/sec
h	Specific enthalpy of g.g. combustion products	BTU/lb
I_o	Inertance in duct, P.U. loop to pump inlet	sec ² /in ²
I_1	Inertance in duct, pump discharge to P.U. loop	sec ² /in ²
I_2	Inertance in duct, P.U. loop to g.g. loop	sec ² /in ²
I_3	Inertance in duct, g.g. loop to thrust chamber	sec ² /in ²
\overline{I}	Moment of inertia of wet turbopump assembly	lb-in-sec ²
I_G	Inertance in duct, g.g. inlet duct	sec ² /in ²
I_L	Inertance in duct P.U. loop duct	sec ² /in ²
I_{TE}	Inertance in duct, gas generator exhaust duct	sec ² /in ²
K_1-K_8	Factors to adjust the magnitudes of forces acting on the structure	-
K_b	Bulk modulus of fluid	lb/in ²
K_b^*	Effective bulk modulus of fluid	lb/in ²
K_{PU}	Factor relating pressure at return end of P.U. loop to pump suction and discharge pressure	-

NOMENCLATURE

SYMBOL	DEFINITION	UNITS
k_g	Total acceleration of launch vehicle	$g's$
k	Factor relating motion of duct wall to a given location	--
L	Inertance of fluid in given length of duct	sec^2/in
L'	Inertance of fluid per unit length of duct	sec^2/in^2
$\bar{l} (=F_L)$	Depth of propellant above tank bottom	in
l	Duct length	in
Me_{qi}	Generalized mass, i^{th} mode	$lb-sec^2/in$
MR	Propellant mixture ratio, thrust chamber	--
MRG	Propellant mixture ratio, gas generator	--
NEI	Number of inboard engines	--
NEO	Number of outboard engines	--
NPSH	Net positive suction head	in
NPSP	Net positive suction pressure	lb/in^2
N_T	Turbine speed	rad/sec
n	Isentropic specific heat ratio	--
P_A	Pressure in feedline at accumulator	lb/in^2
P_B	Pressure in discharge line at g.g. loop junction	lb/in^2
P_C	Thrust chamber pressure	lb/in^2
P_d	Pump discharge pressure	lb/in^2
P_e	Turbine exit pressure	lb/in^2
P_F	Pressure in feedline duct	lb/in^2

NOMENCLATURE

SYMBOL	DESCRIPTION	UNITS
P_g	Pressure in gas generator chamber	lb/in ²
P_i	Turbine inlet pressure	lb/in ²
P_L	Pressure at P.U. loop junction in discharge line	lb/in ²
P_n	Pressure in thrust nozzle at point of gas generator exhaust dump	lb/in ²
P_o	Pressure in duct at junction of feedline segments 1 and 2	lb/in ²
P_S	Pressure at pump inlet	lb/in ²
P_{SL}	Pressure in duct at return point of P.U. loop	lb/in ²
\overline{P}_T	Turbine power	in-lb/sec
P_{TB}	Pressure in feedline duct at tank bottom	lb/in ²
\hat{P}_{TB_i}	Modal tank bottom pressure, i^{th} mode	psi/in
P_{td}	Static pressure in nozzle at the point of turbine exhaust dump	lb/in ²
P_V	Vapor pressure	lb/in ²
q_i	Modal displacement, i^{th} mode	in
Q_i	Generalized force, i^{th} mode	lb
Q_{iLCS}	Generalized force, due to lateral control system, i^{th} mode	lb
Q_{iPERT}	Generalized force due to external perturbation, i^{th} mode	lb
R_0	Resistance in duct, P.U. loop to pump inlet	sec/in ²

NOMENCLATURE

SYMBOL	DESCRIPTION	UNITS
R_1	Resistance in duct, pump discharge to P.U. loop	sec/in ²
R_2	Resistance in duct, P.U. loop to g.g. loop	sec/in ²
R_3	Resistance in duct, g.g. loop to thrust chamber	sec/in ²
R_G	Resistance in duct, g.g. inlet duct	sec/in ²
R_L	Resistance in duct, P.U. loop duct	sec/in ²
R_{TE}	Resistance in duct, gas generator exhaust duct	sec/in ²
T	Engine thrust	lb
$T(\beta c)$	Actuator transfer function	--
T_e	Isentropic turbine exit temperature	°R
T_g	Gas generator chamber temperature	°R
T_i	Turbine inlet temperature	°R
T_{I1}	Longitudinal thrust, inboard engine	lb
T_{I2}	Lateral thrust, inboard engine	lb
T_{O1}	Longitudinal thrust, outboard engine	lb
T_{O2}	Lateral thrust, outboard engine	lb
T_T	Turbine torque	in/lb
T_{NOM}	Nominal thrust of one engine	lb
V_c	Volume of combustion chamber (to throat plane)	in ³
V_g	Volume of g.g. chamber, including torus at turbine inlet	in ³
\dot{w}_2	Flow rate between P.U. loop and g.g. loop junctions	lb/sec

NOMENCLATURE

SYMBOL	DESCRIPTION	UNITS
\dot{w}_3	Flow rate, g.g. loop junction to engine chamber	lb/sec
\dot{w}_c	Flow rate into thrust chamber	lb/sec
\dot{w}_d	Flow rate, pump discharge	lb/sec
\dot{w}_F	Flow rate in duct	lb/sec
\dot{w}_g	Flow rate into gas generator	lb/sec
\dot{w}_L	Flow rate in P.U. loop	lb/sec
\dot{w}_s	Flow rate, pump inlet	lb/sec
\dot{w}_{s1}	Flow rate upstream of return duct of P.U. loop	lb/sec
\dot{w}_{TB}	Flow rate in duct at tank bottom	lb/sec
\dot{w}_{TE}	Flow rate in turbine exhaust duct	lb/sec
x_A	Displacement of duct at accumulator, axial	in
\ddot{x}_{CG}	Acceleration of launch vehicle c.g.	in/sec ²
x_{GP}	Displacement of gimbal point, axial	in
x_O	Displacement of duct at junction of feedline, axial	in
x_P	Displacement of pump, axial	in
x_{TB}	Displacement of tank bottom at feedline junction, axial	in
x_W	Displacement of feedline duct wall along duct axis	in
β_c	Engine command	radians
β_E	Engine deflection	radians
γ	Modal damping coefficient, i^{th} mode	--
$\Delta \dot{w}$	Difference between pump discharge and suction flowrates	lb/sec

NOMENCLATURE

SYMBOL	DESCRIPTION	UNITS
η	Pump efficiency	
η_T	Turbine mechanical efficiency	
ρ_c	Average gas density in combustion chamber	lb/in ³
ρ_F	Density of fuel	lb/in ³
ρ_O	Density of oxidizer	lb/in ³
$\bar{\Phi}$	Control system pitch attitude	radians
$\dot{\bar{\Phi}}$	Control system pitch altitude rate	rad/sec
ϕ_{1A}	Modal displacement, axial, accumulator	in/in
ϕ_{1GP01}	Modal displacement, axial, outboard eng. G.P.	in/in
ϕ_{1GP02}	Modal displacement, lateral, outboard eng. G.P.	in/in
ϕ_{1GPI1}	Modal displacement, axial, inboard eng. G.P.	in/in
ϕ_{1GPI2}	Modal displacement, lateral, inboard eng. G.P.	in/in
ϕ_{10}	Modal displacement, axial, junction of feedline 1&2	in/in
ϕ_{1P}	Modal displacement, axial, pump	in/in
$\phi_{1T\beta}$	Modal displacement, axial, tank bottom	in/in
ϕ_{1w}	Modal displacement, axial, duct wall	in/in
ω_i	Natural frequency of i^{th} structural mode	rad/sec
$\partial h_{TI} / \partial p_g$	Transfer function relating h_{TI} to p_g	BTU/lb-psi
$\partial C_F / \partial P_C$	Transfer function relating C_F to P_C	1/psi
$\partial T_g / \partial MRG$	Transfer function relating T_g to MRG	°R

NOMENCLATURE

SYMBOL	DESCRIPTION	UNITS
$\partial T_g / \partial P_g$	Transfer function relating T_g to P_g	$^{\circ}R/psi$
$\partial C^* / \partial \dot{w}_c$	Transfer function relating C^* to \dot{w}_c	in/lb
$\partial C^* / \partial MR$	Transfer function relating C^* to MR	in/sec
$\partial C_g^* / \partial \dot{w}_c$	Transfer function relating C_g^* to \dot{w}_c	in/lb
$\partial C_g^* / \partial MR$	Transfer function relating C_g^* to MR	in/sec
$\partial (P_d - P_s) / \partial P_s$	Static pump head gain	---
$\partial (P_d - P_s) / \partial \dot{w}_d$	Pump resistance	sec/in
$\partial (P_d - P_s) / \partial N_T$	Transfer function relating pressures to N_T	lb/psi-rad
$\frac{\partial}{\partial w} \left(\frac{1}{K} \right) w$	Pump cavitation frequency factor	in ⁵ /lb
$(\partial V / \partial P_L)$	Polytropic influence coefficient of cavitation bubble	in ⁵ /lb

SUBSCRIPTS

FI	Fuel duct, inboard engine
FO	Fuel duct, outboard engine
OI	Oxidizer duct, inboard engine
OO	Oxidizer duct, outboard engine
i	i th mode
F	Fuel
O	Oxidizer
FTI	Fuel turbine inlet
FTE	Fuel turbine exit
OTI	Oxidizer turbine inlet
OTE	Oxidizer turbine outlet
r	relative
xLAT, yLAT	lateral direction

SUPERSCRIPITS

o	Nominal steady state value
-	Total value (nominal plus perturbation)

1.0 INTRODUCTION

Since the initial launchings of liquid propelled rockets in the late 1950's, the occurrence of longitudinal oscillations somewhere in the structure during certain portions of powered flight have been observed. These have shown up on such launch vehicles as the Thor, Atlas, Titan series, and Saturn series vehicles. Extensive studies have been conducted over the past several years by both government and aerospace industry teams to identify, isolate, remedy, and eliminate this problem, which has become known as the POGO problem. Several of the studies involving POGO analyses are given in the references (Section 5.0).

POGO is a self excited, closed loop phenomenon. It occurs without the excitations associated with appreciable external forcing functions such as wind gusts or launch environments. It is caused by certain interactions involving the vehicle structure, propellant feedlines, propellant pumps, and the propulsion system. For example, a slight perturbation in the thrust of an engine may occur. This causes a structural oscillation which may be felt as a change in tank bottom pressure at the propellant feedline junction. This pressure oscillation at the upper end of the feedline travels down the duct and is felt as pressure and flowrate oscillations at the pump inlet. In turn, these variations in pressure and flowrate feed through the propulsion system and cause additional thrust perturbations, which closes the loop.

These interactions between the various subsystems have been studied by several investigators. The majority of these efforts have been to develop the governing equations of motion and to perform stability analyses at a point in time, for specific launch vehicles.

The purpose of the present contract has been to formulate the equations of motion, and to develop a computer program in the time domain to describe the POGO characteristics of a liquid propelled launch vehicle. It is recognized that significant nonlinearities are present in the overall system, since various flight results have shown these oscillations to buildup, peak, and die down. Other flights have shown continual buildups with no limiting of amplitudes. To predict this type of behavior, the computer program must have the capability to include nonlinear and time-dependent terms.

Such an analytic tool, with minimum dependence upon test results, would be helpful in predicting POGO characteristics of future launch vehicles. This has been the goal of the present contract.

2.0 SUMMARY

This final report contains the results of an effort to predict the POGO characteristics of a typical liquid-propelled launch vehicle. Work was accomplished under contract NAS8-25054 with NASA-MSFC. Volume I of this final report contains the development of the equations of motion of the vehicle and its subsystems.

The subsystems which have been considered include the following:

- a) vehicle structure
- b) lateral control system
- c) propellant feedlines
- d) pump and its associated cavitation phenomena
- e) propulsion system.

Volume II describes the digital computer program which solve the equations developed in Volume I. The program contains time-dependent structural coefficients and non-linear pump cavitation properties. It determines the time response of the vehicle structure and pressure and flow rates throughout the system.

The structural equations are written in modal coordinates, and are the result of a vibration analysis of the entire vehicle. Of prime importance is the modelling of the fluid-tank interaction, which in addition to providing accurate low frequency modal data, also gives the information describing the tank bottom pressure. The modal coefficients are time dependent quantities in the computer program.

Because of structural configuration some vehicles experience coupling between lateral and longitudinal motion. The equations include a lateral control system which monitors vehicle lateral displacements and rotations to initiate lateral thrust components.

Two sets of feedline and propulsion systems are included in the computer program. This corresponds to equivalent outboard and inboard engine systems which are directly applicable to the Saturn flight vehicles and would apply to any engine configuration which can be described by two sets of engines. Each propulsion system is fed by a single oxidizer feedline and fuel feedline, with individual pumps. The feedline is broken into three segments. The first two segments are used to enable the determination of two feedline frequencies where required. A provision exists for an accumulator device between the second and third feedlines.

Pump cavitation is handled by a single coefficient relating time rate of change of inlet pressure to inlet and discharge flowrates. This coefficient is a non-linear function of the pump inlet pressure. The propulsion system describes the pump, discharge lines, propellant utilization loop, thrust chamber and gas generator processes.

The program generated is an analytical tool. However, the pump cavitation process cannot yet be defined analytically, and test data is required to establish levels of cavitation coefficients. In addition, propulsion systems can be described analytically and are treated as such in this report. However, test data is often used to describe the various transfer functions associated with engine performance. The propulsion inputs for this program may be generated analytically or may come from test information.

3.0 Derivation of Equations

3.1 Introduction

The investigation of structural oscillations in a launch vehicle requires knowledge of the structural behavior of the vehicle, the control system employed, the lines feeding the propellants from the structure (tanks) to the turbopumps, and the propulsion system. In the sections which follow, the governing equations are developed from basic fundamentals. The subsystems considered are:

- a. Vehicle structure
- b. Lateral control system
- c. Propellant feedlines
- d. Pump cavitation
- e. Propulsion system

3.2 STRUCTURE

3.2.1 Introduction

The structures subsystem is composed of a set of equations which describe the motion of the structure under certain prescribed external forces. The actual structure must be simulated by a mathematical model which will adequately describe its motion under the influence of the forcing functions which are transient in nature. The structural model must include all flexibilities and load-carrying paths existing in the actual vehicle. Depending on the vehicle under consideration, the model may have to include pitch and/or yaw motions in addition to the longitudinal motion. Frequently, however, a description of only the longitudinal motion is sufficient to adequately model a particular structure. This requires judgement and experience on the part of the analyst.

Local structural components which tend to exhibit motion different than the rest of the vehicle or which should be inspected with more detail (perhaps with a parameter study) may advantageously be handled separately as a branch system to the main structure. Examples are the thrust cross beam structure on the S-II stage of the Saturn vehicles, payload structures, or pump and engine structures which may have unique motions of their own due to either their own structural design or the support system.

Such subsystems can readily be analyzed as separate structures and then coupled into the main structure to form the total structural system.

The analytical approach used in most POGO studies is to obtain the modal equations of motion of the structure rather than use the discrete coordinates to describe motion of the system. The obvious advantage of this approach is that a relatively few modal equations are required to adequately describe the motion of given locations, while using discrete representation necessitates using the equations of motions for all discrete points in the structure. For large launch vehicles, the modal approach would typically use from perhaps one to several equations while a discrete representation would require hundreds of equations.

Another advantage of the modal approach is that modal damping properties are obtainable from structural tests and may be utilized directly in the modal equations of motion. In addition, modal coupling analytical techniques may be applied to handle the branch masses, local structure, or individual stages of a vehicle, discussed above.

Individual stages of a launch vehicle may be treated separately and results coupled together to form the total combined structure. This approach may be advantageous if a given

stage, or given local structure, is undergoing structural modification studies or if test results are being generated to produce mass, stiffness, or damping characteristics of the substructure.

3.2.2 Structural Equations of Motion

The equations of motion of the structural system are written below in matrix notation. Table 3.1.1 presents the nomenclature used.

$$m \ddot{y} + C \dot{y} + \bar{k} y = F$$

As explained above, the solution is formulated in terms of modal coordinates. This is done by expressing the discrete motion as

$$y = \phi q$$

The resulting equations of motion are

$$m\phi\ddot{q} + C\phi\dot{q} + \bar{k}\phi q = F$$

or

$$\phi^T m \phi \ddot{q} + \phi^T C \phi \dot{q} + \phi^T \bar{k} \phi q = \phi^T F$$

For the i th mode, normalizing on $\phi_i^T m \phi_i = M e q_i$, $\phi_i^T C \phi_i$ is approximated by $2 \gamma_i \omega_i M e q_i$ and $\phi_i^T \bar{k} \phi_i = \omega_i^2 M e q_i$.

Thus

$$\ddot{q}_i + 2 \gamma_i \omega_i \dot{q}_i + \omega_i^2 q_i = \phi_i^T F / M e q_i$$

This is the generalized matrix modal equation of the system. Each modal equation is uncoupled from the others. The ω and ϕ values are obtained using standard vibration analysis techniques. The damping values γ are normally obtained from tests or other logical approach.

To handle branch systems, as discussed previously, a modal coupling procedure is used. This is performed as follows.

The branch system (payload structure, for example) is attached to the main structure at a given location A.

TABLE 3.1.1

NOMENCLATURE FOR STRUCTURAL MATRIX EQUATIONS

Subscript M	Main structure
Subscript B	Branch structure
m_M	Mass matrix of the main structure, with branch total mass included at attach point
m_B	Mass matrix of branch structure
\ddot{y}, \dot{y}, y	Acceleration, velocities, and displacements of the discrete panel points used to describe motion of the structure
C	Discrete damping matrix
\bar{k}	Stiffness matrix
F	External forces acting on the structure
q	Generalized coordinate
ϕ	Normalized mode shapes
γ_i	Modal damping ratio of the ith mode
ω_i	Natural frequency of the ith mode
Meq_i	Generalized mass of the ith mode

The equations of motion of the total system (branch structure and main structure) are expressed as

$$\begin{bmatrix} m_B & \\ & m_M \end{bmatrix} \begin{Bmatrix} \ddot{y}_B \\ \ddot{y}_M \end{Bmatrix} + \begin{bmatrix} C_B & \\ & C_M \end{bmatrix} \begin{Bmatrix} \dot{y}_B \\ \dot{y}_M \end{Bmatrix} + \begin{bmatrix} K & \\ & K \end{bmatrix} \begin{Bmatrix} y_B \\ y_M \end{Bmatrix} = \begin{Bmatrix} F \\ F \end{Bmatrix}$$

Let

$$\begin{Bmatrix} y_B \\ y_M \end{Bmatrix} = \begin{bmatrix} \phi_B & \phi_{BM} \\ & \phi_M \end{bmatrix} \begin{Bmatrix} q_B \\ q_M \end{Bmatrix} = [\phi_1] \{q\}$$

The mode shapes chosen for the modal transformation are ϕ_B , ϕ_{BM} , and ϕ_M . The ϕ_B values are obtained from a vibration analysis of the branch system alone, cantilevered at point A. The ϕ_M values are obtained from a vibration analysis of the main structure with the mass of the branch structure lumped at the attachment point A. These separate vibration analysis will produce ω_B and ω_M values as well. The ϕ_{BM} is a set of mode shapes assuming the branch structure to be rigid, and moving in relation to the attach point A. Using this coordinate transformation, the equations of motion become

$$\begin{aligned} [M_C] \begin{Bmatrix} \ddot{q}_B \\ \ddot{q}_M \end{Bmatrix} + \begin{bmatrix} 2\gamma_B \omega_B & \\ & 2\gamma_M \omega_M \end{bmatrix} \begin{Bmatrix} \dot{q}_B \\ \dot{q}_M \end{Bmatrix} \\ + \begin{bmatrix} \omega_B^2 & \\ & \omega_M^2 \end{bmatrix} \begin{Bmatrix} q_B \\ q_M \end{Bmatrix} = \phi_1' F \end{aligned}$$

Hence, M_C is the coupled mass matrix. The modal damping matrix is approximated by uncoupled damping terms. The equations may be written as

$$M_C \ddot{q} + D_C \dot{q} + K_C q = \phi_1' F$$

This is the new equation of motion for the coupled system which includes both main structure and branch structure. The coupled vibration characteristics are obtained by incorporating an additional transformation matrix

$$q = \phi_c q_c$$

and again using standard techniques to obtain the mode shapes (ϕ_c) and the natural frequencies (ω_c). The final coupled modal equations are

$$\ddot{q}_c + 2 \gamma_c \omega_c \dot{q}_c + \omega_c^2 q_c = \phi_c' \phi_1' F$$

The coupled damping terms $2\gamma_c \omega_c$ are obtained from

$$\phi_c' D \phi_c = \phi_c' \begin{bmatrix} 2 \gamma_B \omega_B & | \\ \hline & 2 \gamma_M \omega_M \end{bmatrix} \phi_c = \begin{bmatrix} 2 \gamma_c \omega_c \\ \diagdown \end{bmatrix}$$

Here again, off diagonal terms are generally negligible compared to the diagonal terms and may be neglected. Using this approach, it is seen that damping values of individual modes, either in the branch structure or the main structure, may be varied individually without affecting the overall equations. This is also true of mass and stiffness variations within a branch or main structure. This saves machine computation time because only a portion of the required input need be regenerated due to a change in the branch structure. This also facilitates parameter studies, for example, varying modal damping in the branch.

The motions of the discrete system are obtained from

$$y = \phi_1 q = \phi_1 \phi_c q_c$$

and

$$\ddot{y} = \phi_1 \phi_c \ddot{q}_c$$

The above discussion presents only one method of obtaining the modal characteristics of the vehicle being studied. The important goal to be reaching for is to model the structure in such a way that changes to the basic model may be made with a minimum of complexity. Two extremely vital areas which must be considered are the fluid-tank coupling and the propellant feedline representations. By treating the feedlines as a separate subsystem, it has an interface with the structure, and the structure modeling must reflect this coupling. Care must be exercised so that the feedlines are not included twice in the analysis and that the interface conditions are prescribed correctly. The fluid-tank modeling directly affects the modal characteristics of the vehicle as a whole and directly affects the motion of the tank-propellant feedline junction. The relative importance of this motion upon overall POGO response should be investigated through a parameter study.

3.2.3 Generalized Forces

The Q_i term in the structural equations of motion accounts for all of the external forces acting upon the structure. Since the propellant feedlines have been removed from the structure and treated separately, the forces on the structure due to the feedlines are included as external forces. For the case of lateral-longitudinal coupling, lateral forces are also included. These appear as the lateral component of the engine thrust.

Two engine systems are being considered here, outboard and inboard engines. Only the outboard system is assumed to exert any net lateral thrust on the structure. The inboard system is considered to produce only longitudinal thrust.

As a result, the total generalized force in the i th mode is

$$Q_i = Q_{iA} + Q_{iL} + Q_{iPERT}$$

where

Q_{iA} = axial component of generalized force

Q_{iL} = lateral component of generalized force

Q_{iPERT} = generalized force due to an external excitation
(to start a perturbation to the system, for
response studies)

The components of the generalized force are given as:

$$Q_{iA} = (NEO) [\phi_{iGP01} T_{01} + (\phi_i AP)_{TB00} + (\phi_i AP)_{TBFO} \\ - K_5 (\phi_i AP)_{S00} - K_6 (\phi_i AP)_{SFO}]$$

$$+ (NEI) [\phi_{iGPI1} T_{I1} + \phi_{iGPI2} T_{I2} + (\phi_i AP)_{TB0I} + (\phi_i AP)_{TBF} \\ - K_7 (\phi_i AP)_{S0I} - K_8 (\phi_i AP)_{SFI}]$$

$$Q_{iL} = (NEO) \phi_{GP02} \sin \beta E (T_0 + T_{NOM})$$

Here

- NEO = number of outboard engines
- NEI = number of inboard engines
- ϕ_{ix} = i^{th} modal displacement at location X
- T = engine thrust
- A = feedline duct area
- P = fluid pressure
- K = factor to adjust the magnitude of force acting on structure
- β = outboard engine deflection from zero position.

The tank bottom pressure may be expressed in two ways, as a function of tank bottom axial acceleration or as a function of a modal tank bottom pressure. The latter method requires a structural model which will produce this information, and depends heavily on the propellant-tank representation. Tank bottom pressure is thus defined as

$$P_{TB} = (\text{PMD}) \sum_{i=1}^n (\hat{P}_{TBi}) q_i + \left[\frac{(\text{PAC}) \text{ kg } \rho F_L}{g} \sum_{i=1}^n \phi_{iTB} \ddot{q}_i \right]$$

where

PMD = 1.0 and PAC = 0.0 if P_{TB} is a function of modal tank bottom pressure

PMD = 0.0 and PAC = 1.0 if P_{TB} is a function of tank bottom acceleration

\hat{P}_{TB} = modal tank bottom pressure

kg = launch vehicle acceleration

ρ = propellant density

F_L = height of propellant fluid in tank, surface to feedline junction.

3.3 Lateral Control System

The POGO problem is normally associated with longitudinal oscillations of the launch vehicle. However, with the advent of larger structures, mass and/or stiffness distributions are not necessarily symmetric about the longitudinal axis of the vehicle. Under these conditions, structural disturbances in one plane may well produce motions in other planes. External forces, specifically the engine thrust, must therefore be considered in these other planes. The lateral control system is employed to sense lateral motions of the structure during flight and initiate changes in the thrust vector direction to maintain controlled flight.

A typical lateral control system measures combinations of accelerations, velocities, displacements, slopes, and slope changes at specified vehicle locations. It utilizes this information to produce the engine angular deflection required to stabilize the flight.

The angular motions and rates of motions at specific vehicle locations are expressed as

$$\Phi = \text{angular motion} = \sum_{i=1} \phi_{iCA} \quad q_i, \text{ radians}$$

$$\dot{\Phi} = \text{angular rate} = \sum_{i=1} \phi_{iCR} \quad \dot{q}_i, \text{ radians/sec}$$

where ϕ_{iCA} = modal slope at position measuring vehicle attitude
 ϕ_{iCR} = modal slope at position measuring vehicle attitude rate

This information is generally obtained in both pitch and yaw planes. Often the coupling in only one plane is pronounced, and is adequate to describe the coupled effects.

The control system uses the attitude and attitude rate information to generate an engine command angle β_c , which is given by (for the pitch plane)

$$\beta_c = a_0 F(\Phi) \Phi + a_1 F(\dot{\Phi}) \dot{\Phi}$$

where a_0 and a_1 are the pitch attitude and the pitch attitude rate coefficients, which are set at various values during the course of the flight. $F(\Phi)$ and $F(\dot{\Phi})$ are the pitch attitude and pitch attitude rate error filters, respectively.

These are transfer functions having high order polynomials in both numerator and denominator.

The actual engine angle β_E , is related to the engine command angle β_c by the relation

$$\beta_E = T(\beta_c) \beta_c.$$

This accounts for the dynamics associated with the actuator system. The transfer function $T(\beta_c)$ is also a high order polynomial expression.

For specific applications where only certain frequency ranges are of interest, the order of the polynomial expressions may be reduced significantly to facilitate the solution.

3.4 PROPELLANT FEEDLINES

The propellant feedlines are used to connect the launch vehicle propellant tanks with the pump systems. They are composed of flexible circular ducts of varying cross-sectional areas with bellows, pressure-volume compensators, and orifices located along its length. To describe fluid flow in these ducts, the following assumptions are made:

1. Compressible, one-dimensional, unsteady flow.
2. Velocity profile in the duct is constant with radius at a given cross section.
3. Forces acting in the fluid are viscous forces and inertial forces acting parallel to the flow direction.

Derivation of the governing equations are obtained from the standard fluid dynamic considerations, as typically given in References 1 and 2. This basic approach has been used in past POGO studies such as those presented in References 3, 4, 5, and 6. Equations differences arise in this report because the non-linear expressions have been retained along with the friction and inertial forces. Comparisons with other reports are included.

The mass conservation equation is

$$\frac{\partial}{\partial x} \frac{(\rho u A)}{g} + \frac{\partial}{\partial t} \frac{(\rho A)}{g} = 0 \quad (1)$$

Euler's equation is

$$\frac{\partial}{\partial t} u + u \frac{\partial u}{\partial x} = - \frac{g}{\rho} \frac{\partial p}{\partial x} - \frac{g F_F}{\rho A} + \frac{g F_B}{\rho A} = - \frac{g}{\rho} \frac{\partial p}{\partial x} + \frac{g \bar{F}}{\rho A} \quad (2)$$

For these equations,

F_F = friction force per unit length of duct

F_B = inertia force per unit length of duct

These forces will be expanded later in terms of fluid properties and characteristics.

Euler's equation and the mass conservation equations are combined to form the momentum equation for compressible, viscous, non-steady flow. The resulting expression is

$$\frac{\partial}{\partial t} \frac{(\rho \dot{w} A)}{q} + \frac{\partial}{\partial x} \frac{(\rho u^2 A)}{g} = - A \frac{\partial p}{\partial x} + \bar{F} \quad (3)$$

Equations 1 and 3 are the governing equations of fluid flow through the pipes. These equations will now be put into expressions involving pressures and flow rates.

Equation (1) may be written as

$$\frac{\partial \dot{w}}{\partial x} + \rho \frac{\partial A}{\partial t} + A \frac{\partial \rho}{\partial t} = 0$$

since $\dot{w} = \rho A u$

Further expansion gives

$$\frac{\partial \dot{w}}{\partial x} + \frac{\partial p}{\partial t} \left[\rho \frac{\partial A}{\partial p} + A \frac{\partial \rho}{\partial p} \right] = 0 \quad (4)$$

The area changes with pressure because of the duct wall flexibility. Assuming a uniform duct, free to expand radially under an internal pressure, the duct wall experiences a radial increase δ equal to

$$\delta = \frac{\Delta p R_i^2}{Eh}$$

where

Δp = pressure change

R_i = internal radius

E = Young's modulus of elasticity

h = duct wall thickness

In terms of change of internal cross-sectional area

$$\frac{\partial A}{\partial p} = \frac{\Delta A}{\Delta p} = \frac{2A}{E(D_o - 1) \frac{D_o}{D_i}} = \frac{A}{K_{bd}} \quad (5)$$

The $\frac{\partial \rho}{\partial p}$ term is dependent upon the compressibility of the fluid.

The bulk modulus E_b of the fluid is determined from

$$E_b = \frac{dp}{d\rho/\rho}$$

so that

$$\frac{dp}{d\rho} = \frac{Eb}{\rho} \quad (6)$$

Equation 4 may thus be written as

$$\frac{\partial \dot{w}}{\partial x} + \frac{\partial p}{\partial t} \left[\rho \frac{A}{K_{bd}} + \frac{A\rho}{E_b} \right] = 0$$

or

$$\boxed{\frac{\partial \dot{w}}{\partial x} + \frac{\rho A}{K'_b} \frac{\partial p}{\partial t} = 0} \quad (7)$$

where K'_b is defined as the effective bulk modulus

$$\frac{1}{K'_b} = \frac{1}{K_{bd}} + \frac{1}{E_b} \quad (8)$$

Equation 7 is the final form of the mass conservation equation. It is identical to the corresponding equations in References 4 and 6.

The momentum equation 3 is rearranged to

$$\frac{1}{g} \frac{\partial \dot{w}}{\partial t} + A \frac{\partial p}{\partial x} - \bar{F} = - \frac{1}{g} \frac{\partial}{\partial x} (\rho \dot{w}^2 A)$$

Now,

$$\begin{aligned} \frac{\partial}{\partial x} (\rho u^2 A) &= \frac{\partial}{\partial x} \dot{w} \frac{\dot{w}}{\rho A} = \frac{\partial}{\partial x} \frac{\dot{w}^2}{\rho A} = \frac{1}{\rho A} \frac{\partial}{\partial x} \dot{w}^2 + \dot{w}^2 \frac{\partial}{\partial x} \left(\frac{1}{\rho A} \right) \\ &= \frac{2\dot{w}}{\rho A} \frac{\partial \dot{w}}{\partial x} + \frac{\dot{w}^2}{\rho} \frac{\partial}{\partial x} \left(\frac{1}{A} \right) + \frac{\dot{w}^2}{A} \frac{\partial}{\partial x} \left(\frac{1}{\rho} \right) \end{aligned}$$

$$\frac{\partial}{\partial x} \left(\frac{1}{A} \right) = \frac{\partial}{\partial A} \left(\frac{1}{A} \right) \frac{\partial A}{\partial x} = - \frac{1}{A^2} \frac{\partial A}{\partial p} \frac{\partial p}{\partial x} = - \frac{1}{A^2} \frac{A}{K_{bd}} \frac{\partial p}{\partial x}$$

$$\frac{\partial}{\partial x} \left(\frac{1}{\rho} \right) = \frac{\partial}{\partial \rho} \left(\frac{1}{\rho} \right) \frac{\partial \rho}{\partial x} = - \frac{1}{\rho^2} \frac{\partial \rho}{\partial p} \frac{\partial p}{\partial x} = - \frac{1}{\rho^2} \frac{\rho}{E} \frac{\partial p}{\partial x}$$

Therefore,

$$\frac{\partial}{\partial x} (\rho u A) = \frac{2\dot{w}}{\rho A} \frac{\partial \dot{w}}{\partial x} + \frac{\dot{w}^2}{\rho} \left[- \frac{1}{A} \frac{1}{K_{bd}} \frac{\partial p}{\partial x} \right] + \frac{\dot{w}^2}{A} \left[- \frac{1}{\rho E} \frac{\partial p}{\partial x} \right]$$

$$\begin{aligned}
& - \frac{2\dot{w}}{\rho A} \frac{\partial \dot{w}}{\partial x} + \frac{\dot{w}^2}{\partial A} \frac{\partial p}{\partial x} \left[- \frac{1}{K_{b_d}} - \frac{1}{E} \right] \\
& = \frac{2\dot{w}}{\rho A} \frac{\partial \dot{w}}{\partial x} - \frac{\dot{w}^2}{\rho A K'_b} \frac{\partial p}{\partial x}
\end{aligned}$$

So,

$$\frac{1}{g} \frac{\partial \dot{w}}{\partial t} + A \frac{\partial p}{\partial x} - \bar{F} = - \frac{2\dot{w}}{g \rho A} \frac{\partial \dot{w}}{\partial x} + \frac{\dot{w}^2}{g \rho A K'_b} \frac{\partial p}{\partial x}$$

Dividing by A and defining $L' = \frac{1}{gA}$

$$\boxed{L' \frac{\partial \dot{w}}{\partial t} + \frac{\partial p}{\partial x} \left[1 - \frac{g(L' \dot{w})^2}{\rho K'_b} \right] = - \frac{2L'}{A \rho} \dot{w} \frac{\partial \dot{w}}{\partial x} + \frac{\bar{F}}{A}} \quad (9)$$

Equation 9 is the momentum equation in terms of pressures and flow rates. Elimination of the non-linear terms will reduce this equation to the form found in References 4 and 6 which are linear expressions.

The forces comprising \bar{F} in Equations 2 and 3 are the viscous friction force F_F and the inertial force F_B .

The friction force has the form

$$F_T = F_{ss} + F_F = \frac{1}{2} \frac{\rho}{g} C_f V_T^2 A_d$$

where

F_T = total friction force per unit length of duct

F_{ss} = mean friction force per unit length of duct

F_F = perturbation part of friction force per unit length of duct

C_f = duct friction loss coefficient per unit length

V_T = total fluid velocity relative to duct wall

A_d = duct cross-sectional area

$$V_T = V_{ss} + V_p$$

and

$$F_{ss} = \frac{1}{2} \frac{\rho}{g} C_f V_{ss}^2$$

where

V_{ss} = mean fluid velocity relative to duct wall

V_p = perturbation part of fluid velocity relative to duct wall

In addition,

$$V_{ss} = V + \dot{x}_w$$

and

$$\dot{w} = \rho A_d V$$

where

V = inertial fluid velocity

\dot{x}_w = motion of duct wall along longitudinal axis of duct

\dot{w} = flow rate

Using the above relationships, the perturbation force F_F is

$$F_F = \frac{C_f}{g} V_{ss} (\dot{w} + \rho A_d \dot{x}_w) + \frac{C_f}{2\rho A_d g} (\dot{w} + \rho A_d \dot{x}_w)^2$$

The first term is the linear portion and corresponds to the friction force expression found in Reference 6. The second term is non-linear. Its relative magnitude compared to the linear term is found from

$$1.0 + \frac{(\dot{w} + \rho A_d \dot{x}_w)}{2 V_{ss} \rho A_d}$$

Linear Nonlinear

Inspections of the relative magnitudes of terms, using Titan and Saturn feedlines, have shown that the non-linear term may be neglected.

The inertial force F_B results from the fluid accelerating through the duct. Its magnitude (ignoring local perturbations) is

$$F_B = \frac{\rho A_d}{g} (g + \ddot{x}_{CG}) = kg \rho A_d$$

where \ddot{x}_{CG} is the acceleration of the missile center of gravity.

A flexible connector, such as a bellows in the feedline, may be treated in the same way as flexible feedline itself. The only difference is that the two ends of the connector may move relative to each other. This case has been formulated in Reference 6. The governing equations, including non-linear terms, friction, and inertial forces, are

$$\frac{\partial \dot{w}}{\partial x} + \frac{A_d \rho}{K'_b} \frac{\partial p}{\partial t} = 0$$

$$\frac{\partial p}{\partial x} + L' \frac{\partial \dot{w}}{\partial t} = \rho k g - \frac{C_{fi} V_{oi}}{A_d} (\dot{w} + \rho A_d \dot{x}_{w_{AVE}})$$

$$- \frac{C_{fi}}{2 \rho A_d^2} (\dot{w} + \rho A_d \dot{x}_{w_{AVE}})^2 - \frac{2 L'}{A \rho} \dot{w} \frac{\partial \dot{w}}{\partial x}$$

$\dot{x}_{w_{AVE}}$ = average wall velocity of the connector = $\frac{\dot{x}_{w1} + \dot{x}_{w2}}{2}$

The linearized case, neglecting friction, reduces to

$$\frac{\partial \dot{w}}{\partial x} + \frac{A_d \rho}{K'_b} \frac{\partial p}{\partial t} = 0$$

$$\frac{\partial p}{\partial x} + L' \frac{\partial \dot{w}}{\partial t} = \rho k g$$

which is identical to the presentation in Reference 6.

Reference 6 provides a good description of the formulation for a pressure-volume compensator (PVC). Specifically, a typical PVC may be modeled as a series of three flexible connectors. Thus, the same basic equations developed for the flexible connector apply to the PVC. The boundary conditions between the connectors are expressed by equal pressures and flowrates. Motion between the connectors is defined in terms of the stiffness of the gimbal rings. The final equations are in terms of the pressures, flowrates, and axial displacements at the top and bottom of the PVC.

A study was made to determine the effect of the non-linearities associated with the basic feedlines equations 7 and 9. These two equations are classed as first order quasi-linear partial differential equations of the hyperbolic type. They have the general form:

$$A \frac{\partial \dot{w}}{\partial x} + B \frac{\partial p}{\partial t} = 0$$

$$C \frac{\partial \dot{w}}{\partial t} + D \frac{\partial p}{\partial x} + E \frac{\partial \dot{w}}{\partial x} = F$$

where the two independent variables are x (distance along feedline longitudinal axis) and t (time); the two dependent variables are \dot{w} (perturbated flow rate) and p (perturbated pressure). The coefficients A , B , and C are constants independent of time, space, flow rate, or pressure. Coefficients D and E are a function of flow rate. F represents the inertial and friction forces acting, and is a function of flow rate and feedline motion.

Numerical solution to these equations may be obtained using the method of characteristics, as described in Reference 15. For practical purposes, however, (even such as the long Saturn feedlines), the effect of the non-linear terms are negligible compared to the linear terms, at least for the flow rate perturbations of interest. The feedlines are, therefore, represented by a set of linear equations.

The feedline equations thus have the form

$$A \frac{\partial \dot{w}}{\partial x} + B \frac{\partial p}{\partial t} = 0$$

$$C \frac{\partial \dot{w}}{\partial t} + D \frac{\partial p}{\partial x} = F$$

References 4 and 6 present hyperbolic closed form solutions to these equations. The general equations for pressures and flow rates at location 2 in terms of quantities at location 1 and motions of the feedline boundaries (x_1 and x_2) are, from Reference 6:

$$\begin{Bmatrix} P_2 \\ \dot{w}_2 \end{Bmatrix} = \begin{bmatrix} \cosh X & -Z \sinh X & A_1 & A_2 \\ -\frac{1}{Z} \sinh X & \cosh X & B_1 & B_2 \end{bmatrix} \begin{Bmatrix} P_1 \\ \dot{w}_1 \\ x_1 \\ x_2 \end{Bmatrix}$$

$$x = \gamma \ell$$

$$\gamma = \frac{S}{a} \left[1 + \frac{C_{f1} V_{o1}}{S} \right]^{1/2}$$

$$Z = \frac{\gamma a}{S A g}$$

$$A_1 = \rho k g \cosh X - \beta k S Z \sinh X$$

$$A_2 = -\rho k g - \beta S(1-k) Z \sinh X$$

$$B_1 = -\rho k g \frac{1}{Z} \sinh X - \beta S k (1 - \cosh X)$$

$$B_2 = -S \beta (1-k) (1 - \cosh X)$$

$$\ell = \text{feedline length}$$

$$S = \text{Laplace transform variable}$$

$$a = \text{speed of sound in fluid}$$

$$C_{fi} = \text{feedline wall friction coefficient}$$

$$V_{oi} = \text{mean propellant flow velocity relative to wall}$$

$$\rho = \text{propellant density}$$

$$kg = \text{total vehicle acceleration (1 + inertial acceleration)}$$

$$k = 1.0 \text{ if feedline moves with } x_1 \text{ motion}$$

$$= 0.0 \text{ if feedline moves with } x_2 \text{ motion}$$

$$\beta = \frac{\rho AB}{S+B}$$

$$A = \text{feedline area}$$

$$B = C_{fi} V_{oi}$$

The hyperbolic terms have been expanded into their series form.

$$\cosh X = 1 + \frac{\gamma^2 \ell^2}{2} + \frac{\gamma^4 \ell^4}{24} + \dots$$

$$Z \sinh X = \frac{\ell}{Ag} [S+B] \left(1 + \frac{\gamma^2 \ell^2}{6} + \frac{\gamma^4 \ell^4}{120} + \dots \right)$$

$$\frac{1}{Z} \sinh X = \frac{A \ell g s}{a^2} \left(1 + \frac{\gamma^2 \ell^2}{6} + \frac{\gamma^4 \ell^4}{120} + \dots \right)$$

Expressing these functions in terms of the transform variable, and keeping up to second order terms,

$$\cosh X = 1 + \left(\frac{\ell^2 B}{a^2 2} \right) S + \left[\frac{\ell^2}{a^2} \left(\frac{1}{2} + \frac{B^2}{24} \right) \right] s^2$$

$$Z \sinh X = LB + \left[L \left(1 + \frac{B^2}{6} \frac{\ell^2}{a^2} \right) \right] S + \left[\frac{\ell^2}{a^2} \frac{LB}{3} \left(1 + \frac{B^2}{60} \frac{\ell^2}{a^2} \right) \right] s^2$$

$$\frac{1}{Z} \sinh X = \frac{A g \ell}{a^2} \left[S + \left(\frac{B \ell^2}{2 a^2} \right) s^2 \right]$$

where $L = \text{inertance of fluid in duct, } = \frac{\ell}{A g}$.

For the case where the length of the feedline duct is relatively small, such that the term ℓ^2/a^2 is small, the hyperbolic functions are approximated by

$$\cosh X = 1$$

$$Z \sinh X = LB + LS$$

$$\frac{1}{Z} \sinh X = 0$$

The feedline equations become

$$\begin{bmatrix} p_2 \\ \dot{w}_2 \end{bmatrix} = \begin{bmatrix} 1 & -(LB+LS) & \rho k g - \beta k s (LB+LS) & -\rho k g - \beta (1-k) s (LB+LS) \\ 0 & 1 & 0 & 0 \end{bmatrix} \begin{bmatrix} p_1 \\ \dot{w}_1 \\ x_1 \\ x_2 \end{bmatrix}$$

The flow rates are in the inertial reference frames. For duct locations where relative flow is important, such as the pump inlet, an additional relationship is used.

$$\dot{w}_{\text{relative}} = \dot{w}_{\text{inertial}} + \rho A \dot{X}$$

where \dot{X} is the velocity of the feedline location where relative motion is desired.

Accumulator

To eliminate or reduce the POGO problem for a specific flight vehicle, an accumulator type device has been successfully inserted into the feedline system at its lower end, near the pump inlet. Titan, Saturn S-IC, and Saturn S-II stages have applied this fix effectively.

Equations for typical accumulator can be expressed as for a damped single degree of freedom system directly attached to the feedline. Schematically, this appears in Figure as

The equations for this system are

$$P_A = L_A^1 \ddot{w}_A + \frac{R_A^1}{\rho A_A^2} \dot{w}_A + \frac{K_A^1}{\rho A_A^2} w_A$$

$$\text{and } w_1 = w_A + w_2$$

$$\text{where } P_A = P_1 = P_2$$

$$L_A^1 = \text{equivalent inertance of accumulator (sec}^2/\text{in}^2)$$

$$R_A^1 = \text{equivalent discrete damper of accumulator (lb-sec/in)}$$

$$K_A^1 = \text{equivalent spring rate of accumulator (lb/in)}$$

$$A_A = \text{equivalent cross sectional area of accumulator duct (in}^2)$$

a more general expression for the pressure of this junction is

$$P_A = L_A^1 \ddot{w}_A + R_A^1 \dot{w}_A + C_A^1 w_A$$

Using this form, any type of accumulator device approximated by a single degree of freedom system may be used.

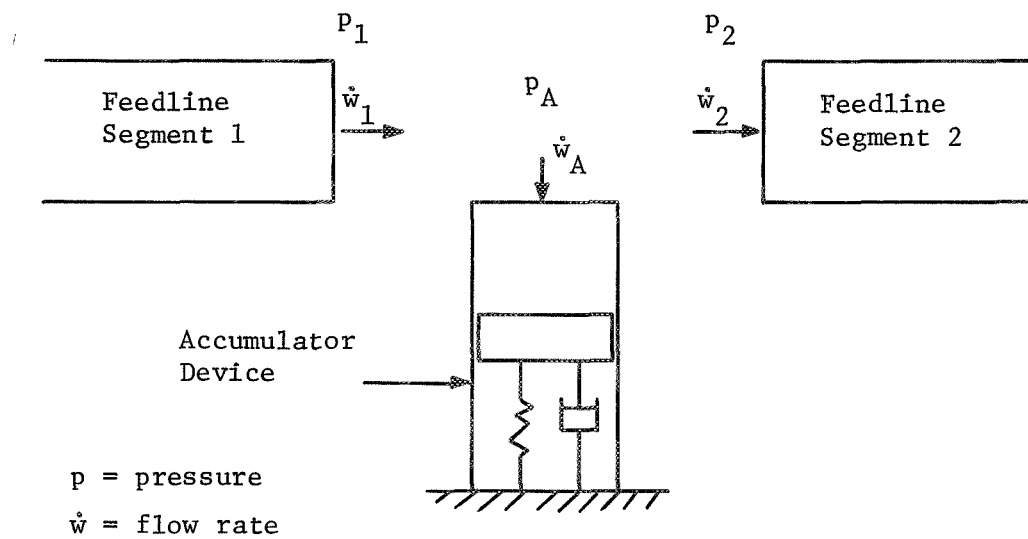


Figure 3.4.1 Accumulator Representation

3.5 Pump Cavitation

The presence of vapor bubbles in or near the pump inlet caused by cavitation of the flowing fluid, is recognized to have a significant effect upon pressure and flow oscillations at this location. Depending on the launch vehicle configuration and feedline geometries, pump cavitation can be the most significant factor in the propagation of the POGO phenomenon.

Cavitation occurs when the pump inlet pressure drops to a certain level, the vapor pressure of the flowing fluid. The amount of cavitation (volume of vapor bubbles) varies with inlet pressure and thus is a non-linear quantity which acts on the system.

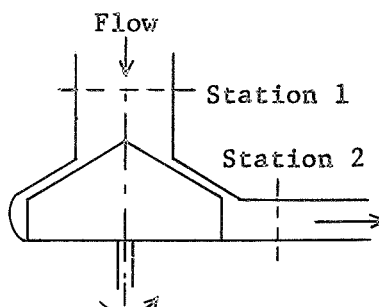
Attempts by various investigators to model the behavior of the cavitation bubble in terms of a single polytropic compression-expansion process have been impaired by the difficulty in treating the phase changes occurring in the cavitation region. The rate of phase change and, therefore, the error introduced into calculating the flexibility coefficient of the bubble is dependent on the time rate of static pressure changes in the cavitation region, i.e., the frequency of pressure oscillations.

Bikle, Fidler, and Rohrs (References 7, 8, 9) performed a detailed study to formulate the procedure to model the cavitation bubble by solving equations of motion of the two phase fluid as it moves through the rotating turbopump. A conformal mapping technique was used to map the pump blade into a flat plate with the hope of solving for the velocity and pressure fields. and, therefore, from thermodynamic considerations arrive at the relative quantities of liquid and vapor in the region of cavitation.

This work is presently being completed under a NASA technology contract to Martin Marietta, Denver Division. The goal of this contract is to analytically simulate the propagation of pressure transients through a turbopump. Results of this study should be directly applicable to POGO analyses on launch vehicles. It will hopefully provide an analytic tool to describe the cavitation effect of a pump where no test data is available.

To provide a simple and reasonably accurate representation of the cavitation bubble, an effort has been made in this present study to superimpose a polytropic behavior of the cavitation bubble with a frequency dependent correction factor. The polytropic relations yield non-linear amplitude dependent spring properties, and the frequency correction factor, determined experimentally for specific configuration and pump liquid, yields a simplified treatment of the dependence of the phase change on the rates of pressure changes in the cavitation region.

Following is the development of the analytic treatment of the cavitation bubble.



Pump Schematic

Figure 3.5.1

Applying mass continuity requirement in the control volume between stations 1 and 2 of Figure 3.5.1 results in

$$\frac{\partial}{\partial x} (\rho u A) = \frac{\partial}{\partial t} (\rho A) = A(x) \frac{\partial \rho}{\partial t}$$

$$\dot{w}_d - \dot{w}_s = g \text{ VOL } \frac{\partial}{\partial t} (\rho_{\text{AVE}}) = \frac{\partial}{\partial t} m(t)$$

- where
- VOL = volume of pump region between stations 1 and 2.
 - ρ_{ave} = average mass density of the two phase flow.
 - $m(t)$ = combined mass of liquid and vapor in the control volume.
 - \dot{w}_s = flow rate upstream of the cavitation bubble.
 - \dot{w}_d = flow rate downstream of the cavitation bubble

In the development of the polytropic relation for the vapor bubble, the following assumptions are made:

1. $dV_{\text{Liquid}} = -dV_{\text{Vapor}}$
2. $\rho_{\text{Liquid}} = \text{constant}$
3. $m_{\text{Vapor}} = \text{constant}$

The combined mass may be written as

$$m(t) = \rho(\text{liquid}) V(\text{liquid}) + \rho(\text{vapor}) V(\text{vapor})$$

using the three assumptions, also,

$$\frac{\partial}{\partial t} m(t) = -\rho(\text{Liquid}) \frac{dV(\text{vapor})}{dp(\text{local})} \frac{dp(\text{local})}{dt}$$

where $p(\text{local})$ is the local static pressure in the cavitation region, and $V(\text{vapor})$ is the volume occupied by the vapor.

The term $dV(\text{vapor})/dp(\text{local})$ may be called the "air spring" flexibility coefficient. Consider the liquid-vapor branch of the phase diagram depicted in Figure 3.5.2. For any cavitation at all to exist in the pump inlet region, local static pressure must be below the vapor pressure of the propellant.

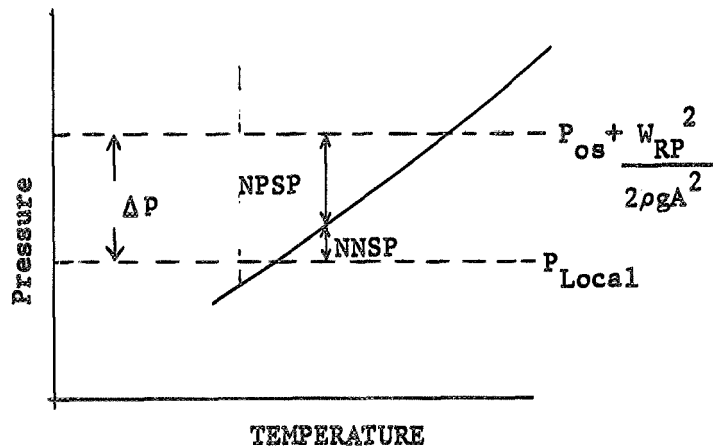


Figure 3.5.2 Vapor Pressure Curve of the Propellant

P_{os} = static pressure at pump inlet

W_{RP} = flowrate relative to pump

P_{Local} = local pressure in cavitation region

NNSP = net negative suction pressure in cavitation region

NPSP = net positive suction pressure

It is, therefore, the "NNSP" which is the driving potential in the cavitation process. The Δp is the reduction of the fluid stream pressure from the level existing just upstream of the pump inlet to the level existing in cavitation region. This Δp depends on pump geometry, pump radial velocity, and the fluid characteristics, to the first approximation. Assuming Δp to be constant for the span of

operating conditions of interest, we can express the following

$$P_{\text{Local}} = P_v + \text{NPSP} = \Delta p$$

and

$$dP_{\text{Local}} = d(\text{NPSP})$$

where P_v is the equilibrium vapor pressure of the propellant.

The polytropic relation for the bubble vapor is

$$P_{\text{Local}} V^n = \text{constant}$$

Here, n = polytropic exponent.

Differentiating implicitly and solving for $(\frac{dV}{dp})$, we obtain

$$(\frac{dV}{dp})_p = - \frac{V}{np}$$

Expressing V in terms of P and initial conditions, we obtain

$$(\frac{dV}{dp})_p = - \frac{P_o^{1/n} V_o}{n} \frac{1}{P^k} = A_o \frac{1}{P^k}, \text{ where } k = \left(\frac{1+n}{n}\right)$$

At present the value of A_o must be determined experimentally. Sufficient data are available for most liquid rocket systems to provide the value of A_o .

$$(\frac{dV}{dP})_p = A_o \frac{1}{(P^o + P)^k} = A_o (P_v + \text{NPSP})^{\frac{1}{n} + k}$$

where P^o is the steady state pressure in the cavitation region; P_v is the vapor pressure of the propellant; P is the perturbation portion of the local pressure. For our case, P equals NPSP, where NPSP is the perturbation in net positive suction pressure; and P^o equals P_v .

Thus,

$$(\frac{\partial V}{\partial p})_p = A_o (P_v + \text{NPSP})^{\frac{-(1+n)}{n}}$$

The above expression defines the air spring coefficient in terms of the perturbation in NPSP and the parameters of the propellant and pump. The deviation of the behavior of the cavitation bubble from the polytropic expansion - compression is due to phase change occurring at the liquid - vapor interface. Therefore, the changes in the bubble volume are partly due to polytropic process and partly due to changes in the quantity of vapor involved, i.e. liquification during compression and vaporization during expansion.

The total change in bubble volume is then

$$dV = d(Mv)$$

where M is the mass of vapor, and v is the specific volume of vapor.

$$dV = Mdv + vdM = (dV)_p + vdM$$

The first term represents the polytropic process while the vdM term accounts for the changes in the bubble volume due to changes in vapor mass resulting from the phase change of the propellant.

The expression for the air spring coefficient can be rewritten as

$$\left(\frac{dV}{dp}\right)_{\text{total}} = \left(\frac{dV}{dp}\right)_p + v \frac{dM}{p} = A_o (P_v + \text{NPSP})^{\frac{-(1+n)}{n}} + f(\omega)$$

Transient mass transfer at the liquid - vapor interface of cavitation bubble depends on heat transfer characteristics at the bubble surface, thermodynamic properties of the propellant, and pressure and temperature of the propellant in the cavitation region. Therefore, exact modeling of the mass transfer is extremely difficult to accomplish and the parameters that effect the mass transfer depend either on thermodynamic properties or parameters which vary with time and thus the frequency of the pressure oscillations. A simple modeling of the mass transfer (the second term) can be accomplished by the following expression.

$$f(\omega) = \frac{\partial(1/k)}{\partial\omega} \omega$$

where ω is the radial frequency of pressure oscillations. The term

$$\frac{\partial}{\partial\omega} \left(\frac{1}{K}\right)$$

must be evaluated from system test or flight data. Expressing $\frac{\partial}{\partial\omega} \left(\frac{1}{K}\right)$

in terms of a polynomial in ω , its non-linear characteristics can be included.

From thermodynamic considerations discussed above it is apparent that

$$\lim_{\omega \rightarrow \infty} \left\{ \frac{\partial (1/\bar{k})}{\partial \omega} \right\} \rightarrow 0$$

i.e., the polytropic modeling of the cavitation bubble becomes more accurate with increasing ω .

The continuity equation across the pump can now be rewritten as follows.

$$-\dot{w}_d + \dot{w}_s = \rho_{(\text{Liquid})} (\text{NPSP}) [A_o (P_v + \text{NPSP})^{\frac{-(1+n)}{n}} + \frac{\partial}{\partial \omega} \left(\frac{1}{\bar{k}} \right) \omega] .$$

This can be expressed in a different form as:

$$\dot{w}_s - \dot{w}_d = C_{p1} \dot{p}_s + (C_{p1}) (C_{p3}) \ddot{w}_s + (C_{p1}) (C_{p4}) \dot{w}_s \ddot{w}_s$$

where

$$C_{p1} = \rho A_o [P_v \bar{k} + f(\omega)]$$

$$C_{p2} = \rho A_o \bar{k} p_v^{\bar{k}-1}$$

$$C_{p3} = \left[\frac{\dot{w}_s}{\rho g A_s^2} \right]$$

$$C_{p4} = \frac{1}{\rho g A_s^2}$$

$$\bar{k} = - \frac{(n+1)}{n}$$

In its simplest form, the pump cavitation equation has the familiar form

$$\dot{w}_s - \dot{w}_d = C_{p1} \dot{p}_s$$

3.6 Propulsion System

A schematic of a typical propulsion system is given in Figure 3.6.1. This includes the pump, discharge lines, propellant utilization loop, gas generator circuit, turbine, and the thrust combustion chamber.

3.6.1 Thrust Combustion Chamber

Total engine thrust at time $(t + \Delta t_1)$ is related to chamber pressure by

$$\bar{T}(t + \Delta t_1) = A_T \bar{C}_F(t) \bar{P}_c(t)$$

where Δt_1 is a lag time representing the average dwell time of the combustion products in the chamber.

$$\Delta t_1 \approx \frac{\rho_{AVE} V_c}{\dot{w}_c^o} \quad 1)$$

where ρ_{AVE} = average density of gaseous combustion products in the chamber

V_c = volume of chamber

\dot{w}_c^o = steady state flowrate in chamber

also, A_T = chamber throat area (constant value)

$C_F(t)$ = thrust coefficient at time t , varying with chamber pressure

$P_c(t)$ = chamber pressure at time t

The perturbation portion of total thrust is written as

$$T(t + \Delta t_1) = A_T [C_F^o P_c(t) + C_F(t) P_c^o(t) + C_F(t) P_c(t)] \quad 2)$$

In these equations, superscript "o" denotes steady state values of the involved parameters. The perturbation portion of C_F is

$$C_F = \frac{\partial C_F}{\partial P_c} P_c$$

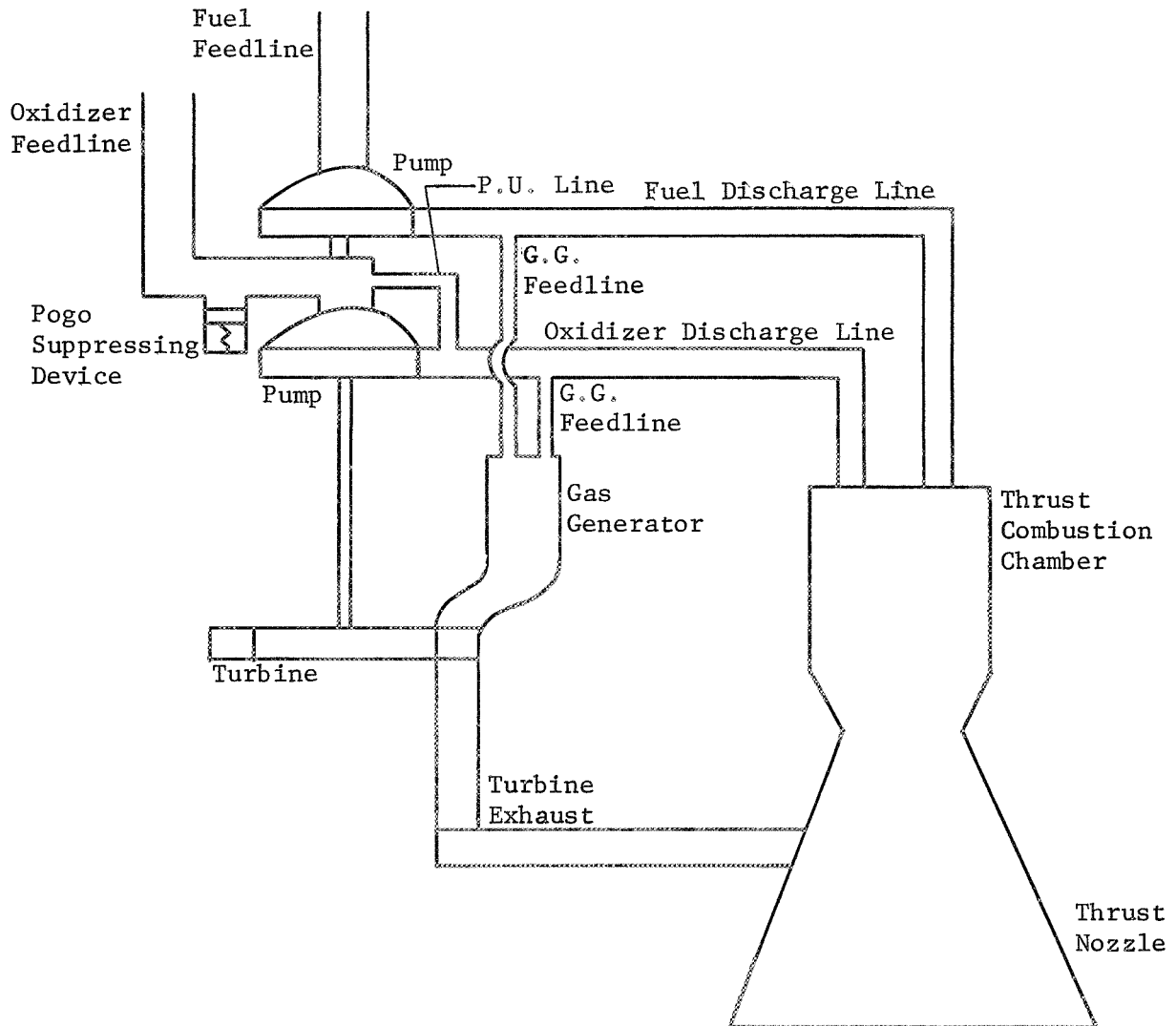


Figure 3.6.1 Typical Propulsion System Schematic

The variation of C_F with P_c is normally available for the given engine by the engine manufacturers. However, it can be determined analytically, using the expressions below, as developed in References 10 and 11.

$$C_F = \left\{ \frac{2}{n-1} \left(\frac{2}{n+1} \right)^{\frac{n+1}{n-1}} \left[1 - \left(\frac{P_e}{P_c} \right)^{\frac{n-1}{n}} \right] \right\}^{1/2} + \frac{(P_e - P_a)}{P_c} \frac{A_e}{A_t} \quad 3)$$

$$\frac{A_t}{A_e} = \left(\frac{n+1}{2} \right)^{1/n-1} \left(\frac{P_e}{P_c} \right)^{1/n} \left\{ \frac{n+1}{n-1} \left[1 - \left(\frac{P_e}{P_c} \right)^{(n-1)/n} \right] \right\}^{1/2} \quad 4)$$

where n = specific heat ratio

P_e = pressure in the exit plane

P_a = ambient pressure

A_e = area of exit plane

A_t = throat area

These are based upon steady flow conditions, perfect gas laws, and isentropic flow through the nozzle.

The total chamber pressure P_c at time t is expressed as

$$P_c(t) = \frac{C^*}{gA_t} \dot{w}_c(t-\Delta t_2) = \frac{C^*}{gA_t} [\dot{w}_{co}(t-\Delta t_2) + \dot{w}_{CF}(t-\Delta t_2)] \quad 5)$$

The time lag Δt_2 represents the average time that propellants dwell in the thrust chamber from the time of injection through vaporization and combustion. Perturbation part of the chamber pressure is (dropping the time subscript for convenience)

$$P_c = \frac{1}{gA_t} [C^{*o} \dot{w}_{co} + C^{*o} \dot{w}_{CF} + C^* \dot{w}_{co}^o + C^* \dot{w}_{CF}^o + C^* \dot{w}_{co} + C^* \dot{w}_{CF}] \quad 6)$$

where A_t = equivalent chamber throat area

C^* = characteristic velocity

\dot{w}_{co} = oxidizer flowrate into the combustion chamber

\dot{w}_{CF} = fuel flowrate into the combustion chamber

Superscript "o" represents steady state values while the other values are perturbation values. The characteristic velocity is generally a function of the mixture ratio MR and total flowrate

into the chamber, \dot{w}_c . This is expressed as

$$C^* = \frac{\partial C^*}{\partial MR} MR + \frac{\partial C^*}{\partial \dot{w}_c} \dot{w}_c \quad 7)$$

This information is normally presented for a given engine system as plots of C^* as functions of mixture ratio and chamber flowrates. Often the second term is negligible and may be ignored.

The perturbation in mixture ratio is found by subtracting steady state value (MR°) from total mixture ratio (MR).

$$MR = \overline{MR} = MR^\circ + \frac{\dot{w}_{co} MR^\circ \dot{w}_{CF}}{\dot{w}_{CF} + \dot{w}_{CF}} \quad 8)$$

Likewise, the perturbation in chamber flow rate is

$$\dot{w}_c = \dot{w}_{co} + \dot{w}_{CF} \quad 9)$$

Introducing these relationships, ignoring the $\frac{\partial C^*}{\partial \dot{w}_c}$ item, and linearizing the remainder of the equations, the chamber pressure equation becomes

$$P_c(t) = \frac{C^* + \frac{\partial C^*}{\partial MR} \left(\frac{\dot{w}_{co}^\circ + \dot{w}_{CF}^\circ}{\dot{w}_{CF}^\circ + \dot{w}_{CF}^\circ} \right)}{gA_c} \dot{w}_{co}(t-\Delta t_2) \quad 10)$$

$$C^* = \frac{\partial C^*}{\partial MR} \dot{w}_{co}^\circ \left(\frac{MR^\circ + 1}{\dot{w}_{CF}^\circ + \dot{w}_{CF}^\circ} \right)$$

$$+ \frac{\dot{w}_{CF}^\circ}{gA_c} \dot{w}_{CF}(t-\Delta t_2)$$

This is essentially the same as the linear results presented, for example, in Reference 12.

The above equations determine the thrust and chamber pressure perturbations from the perturbations in propellant flowrates into the chamber. Quantities Δt_1 , Δt_2 , once determined for a particular propellant combinations and the engine geometry will allow the establishment of the phase between perturbations in flowrates, chamber pressure, and thrust exerted on the chamber nozzle. It must be kept in mind that the flowrates appearing in the expressions for thrust and chamber pressure are the flowrates relative to the chamber.

3.6.2 Turbopump Assembly

a. Gas Generator

The chamber pressure is treated in the same manner as the thrust chamber pressure. The basic relation for the gas generator chamber pressure is the same as equation 5), with the proper subscripts.

The perturbation in the gas generator chamber pressure is identical to equation 10), again using the proper subscripts.

b. Pumps

The perturbation in the turbine brake power is

$$P_T = \eta_T (\dot{H}_{TI} - \dot{H}_{TE})$$

where η_T = turbine mechanical efficiency

\dot{H}_{TE} = turbine exit total enthalpy rate (perturbation)

\dot{H}_{TI} = turbine inlet total enthalpy rate (perturbation)

Turbine brake power (perturbation) is also expressed as

$$P_T = L_T^\circ N_T + N_T^\circ L_T + L_T N_T$$

where N_T = turbine angular velocity

L_T = turbine torque

For the case of both pumps driven by a common turbine,

$$P_T = P_O + P_F$$

where P_O and P_F represent mechanical power delivered to the oxidizer and fuel pumps. The power imparted to the fluid is

$$P_{\text{fluid}} = \eta_O P_O + \eta_F P_F$$

where η_O and η_F are the oxidizer and fuel pump efficiencies. The total power imparted to the oxidizer fluid through the oxidizer pumps, assuming incompressible flow through the inlet and discharge planes of the pump, is

$$P_O = \frac{1}{\rho_O \eta_O} (\bar{\dot{w}}_d \bar{P}_d - \bar{\dot{w}}_s \bar{P}_s)$$

The perturbation portion is

$$P_o = \frac{1}{\rho_o \eta_o} [\dot{w}_{do}^o (P_{do} - P_{do}^o) + (P_{do}^o - P_{so}^o) \dot{w}_{do} + P_{so}^o \Delta \dot{w}_o + \dot{w}_{do} (P_{do} - P_{so}) + P_{so} \Delta \dot{w}_o]$$

$$\Delta \dot{w}_o = \dot{w}_{do} - \dot{w}_{so}$$

An identical expression holds for the fuel pump.

The pump power is also expressed as

$$P_p = N_T^o M_p + M_p^o N_T + N_T M_p$$

for each pump where

M_p = pump torque

Turbine speed will change if the pump torque and the turbine torque are not equal. These are related by

$$I \dot{N}_T = L_T - M_p$$

where I is the moment of inertia of the wet turbopump assembly.

The rise in pressure across the pump (inlet to outlet) is generally affected by changes in the inlet pressure, discharge flow rate, and pump speed. These quantities may be obtained either from analytical sources or from test data. The relationships are expressed by a single equation as

$$(P_d - P_s) = \frac{\partial (P_d - P_s)}{\partial P_s} P_s + \frac{\partial (P_d - P_s)}{\partial \dot{w}_d} \dot{w}_d + \frac{\partial (P_d - P_s)}{\partial N_T} N_T$$

3.6.3 Gas Generator Exhaust Flow

The total enthalpy rate (turbine inlet power) is defined as

$$\dot{H}_{TI} = \dot{w}_g \bar{h}_{(t+\Delta t_3)}$$

where \dot{w}_g = total gas generator flow rate

\bar{h} = total specific enthalpy of combustion products

The time lag Δt_3 is the average vaporization and combustion time, and Δt_4 is the dwell time of gaseous combustion products in the chamber.

$$\Delta t_4 = \frac{\rho_{g,AVE} V_{gg}}{\dot{w}_g^o}$$

where $\rho_{g,AVE}$ = average density of gaseous combustion products in the chamber

V_{gg} = volume of the gas generator chamber

\dot{w}_g^o = steady state flowrate in chamber

Perturbation in total enthalpy rate is

$$\dot{H}_{TI}(t+\Delta t_3+\Delta t_4) = \dot{w}_g^o h(t+\Delta t_3) + h^o(t+\Delta t_3) \dot{w}_g(t) + \dot{w}_g(t) h(t+\Delta t_3)$$

where \dot{w}_g = perturbation part of flowrate in chamber

h = perturbation part of specific enthalpy of combustion products

The value of h is

$$h = C_p T_g + \frac{\partial h}{\partial P_g} P_g$$

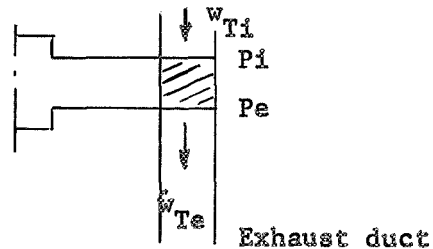
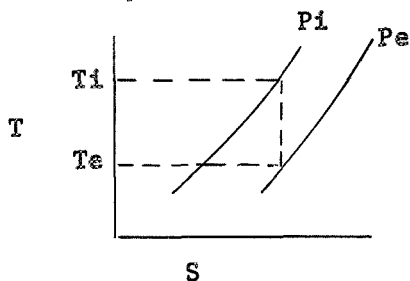
where C_p = specific heat of the liquid

T_g = perturbation portion of gas generator temperature

$$T_{g(t)} = \frac{\partial T_g}{\partial \text{MRG}} \text{MRG}(t+\Delta t_3) + \frac{\partial T_g}{\partial P_g} P_g$$

These equations relate the total enthalpy rate and gas generator pressure in terms of perturbations in the gas generator fuel and oxidizer flowrates.

The gases flowing from the gas generator at high pressures and temperatures drive the turbines to operate the pumps. The assumed isentropic pressure-temperature relationships at the turbine inlet and exit planes are sketched below.



The isentropic flow process is described by

$$\left(\frac{T_e}{T_i}\right) = \left(\frac{P_i}{P_e}\right)^{n/n-1}$$

In this equation

$P_i = P_g$ = perturbation in gas generator chamber pressure

P_e = perturbation in the turbine isentropic exit pressure

T_e = perturbation in the turbine isentropic exit temperature

$T_i = T_g$ = perturbation in gas generator chamber temperature

Assuming $\dot{w}_{T_i} = \dot{w}_{T_e}$, the perturbed total turbine exit enthalpy is

$$\dot{H}_{T_e} = \dot{w}_{T_e}^{\circ} h_{T_e}^{\circ} + h_{T_e}^{\circ} \dot{w}_{T_e} + h_{T_e} \dot{w}_{T_e}$$

$$h_{T_e} = \frac{\partial h_{T_e}}{\partial P_e} P_e + \frac{\partial h_{T_e}}{\partial T_e} T_e$$

The perturbation T_e is

$$T_e = (T_i^{\circ} + T_i) \left(\frac{P_i + P_i^{\circ}}{P_e + P_e^{\circ}} \right)^{n/n-1} - T_e^{\circ}$$

The coefficients described in the preceding subsections of the propulsion system section may be determined experimentally from an existing engine system. These coefficients may also be determined analytically, provided certain information is available. The following subsection describes this approach.

3.6.4 Discharge Line Equations

The flow of propellants aft of the pumps and the flow of gases aft of the gas generator is assumed to be incompressible. The pressure and flow rate terms take the form of

$$P_1 = P_2 + R\dot{w} + I \ddot{w}$$

$$\Sigma \dot{w} \text{ at a junction} = 0.$$

where P_1 is the upstream pressure, P_2 is the downstream pressure, \dot{w} is the flow rate (constant between points 1 and 2), R is the line resistance, and I is the inertance of the fluid in the line section.

The lines considered include

- a. Pump to thrust chamber
- b. Propellant utilization loop (where applicable)
- c. Line to gas generator
- d. Gas generator exhaust lines.

Based on the discharge line system shown in Figure 3.6.2, the equations are

<u>EQUATION</u>	<u>LINE</u>
$P_{SL} = P_s + R_o \dot{w}_s + I_o \ddot{w}_s$	P.U. junction to pump inlet
$P_d = P_L + R_1 \dot{w}_d + I_1 \ddot{w}_d$	Pump to P.U. loop
$P_L = P_B + R_2 \dot{w}_2 + I_2 \ddot{w}_2$	P.U. to gas generator branch
$P_L = P_{SL} + R_L \dot{w}_L + I_L \ddot{w}_L$	P.U. loop
$P_B = P_c + R_3 \dot{w}_3 + I_3 \ddot{w}_3$	G.G. branch to engine chamber
$P_B = P_g + R_g \dot{w}_g + I_g \ddot{w}_g$	Gas generator line
$P_e = P_n + R_{TE} \dot{w}_{TE} + I_{TE} \ddot{w}_{TE}$	Turbine exhaust line

$$\dot{w}_s = \dot{w}_{SL} + \dot{w}_L$$

$$\dot{w}_d = \dot{w}_L + \dot{w}_2$$

$$\dot{w}_2 = \dot{w}_g + \dot{w}_3$$

$$\dot{w}_3 = \dot{w}_c$$

The discharge line equations will vary slightly, depending on the existence of a propellant utilization (P.U.) line, and where the P.U. line junctions are. For example, on the Saturn S-II J-2 engine, the P.U. line begins and ends at essentially the same point...near the pump discharge plane.

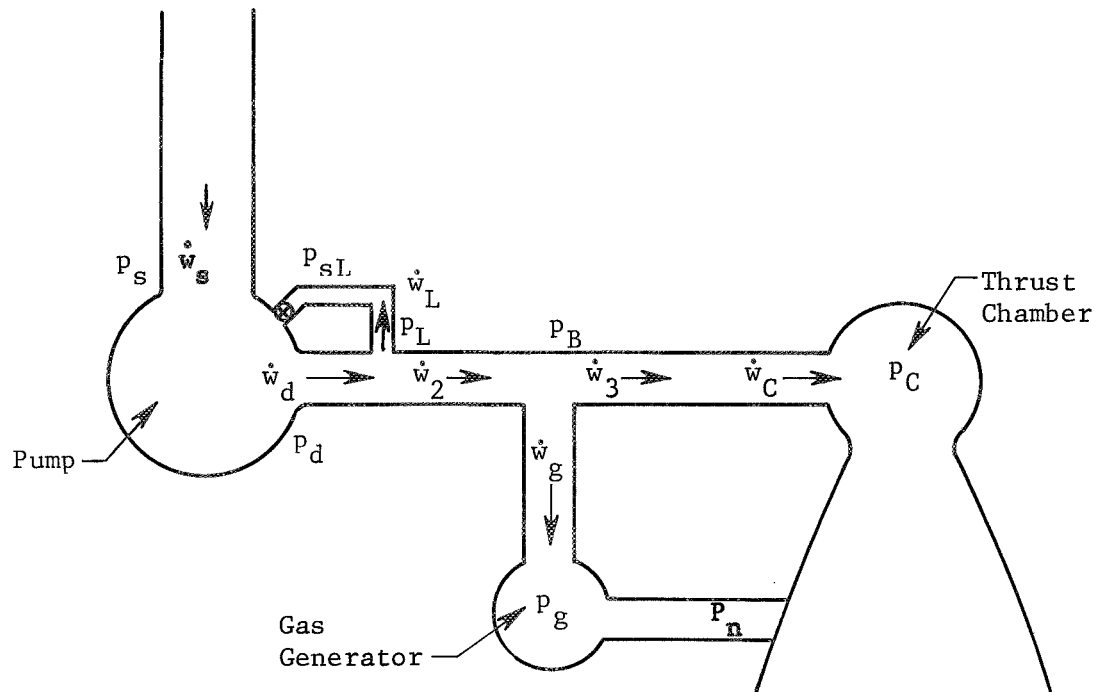


Figure 3.6.2 Typical Propulsion Discharge Line System

4.0 SUMMARY OF EQUATIONS

The equations which have been developed in the previous section are summarized here.

STRUCTURAL EQUATIONS

$$\ddot{q}_i = -2\gamma_i \omega_i \dot{q}_i - \omega_i^2 q_i + \frac{Q_{iA}}{M_{eqi}} + \frac{Q_{iL}}{M_{eqi}} + \frac{Q_{iPERT}}{M_{eqi}}$$

Q_{iA} = generalized force due to axial forces

Q_{iL} = generalized force due to lateral forces

Q_{iPERT} = generalized force due to external excitation

$$Q_{iA} = (\text{NEO}) \left[\phi_{iGPO1} T_{O1} + \left(\phi_{iTB}^A T_{TB}^{P_{TB}} \right)_{OUTB} - \left(K \phi_{iP}^A S_{PS} \right)_{OUTB} \right] \\ + (\text{NEI}) \left[\phi_{iGPI1} T_{I1} + \left(\phi_{iTB}^A T_{TB}^{P_{TB}} \right)_{INB} - \left(K \phi_{iP}^A S_{PS} \right)_{INB} \right]$$

$$Q_{iL} = (\text{NEO}) \phi_{GPO2} \sin \beta_E \left[T_O + \bar{T}_{NOM} \right]$$

$$P_{TB} = K \frac{\rho}{g} \bar{x} \ddot{x}_{TB} \text{ or } P_{TB} = K \sum_{i=1}^n \hat{p}_{iTB} q_i$$

$$x = \sum_{i=1}^n \phi_i q_i$$

$$\dot{x} = \sum_{i=1}^n \phi_i \dot{q}_i$$

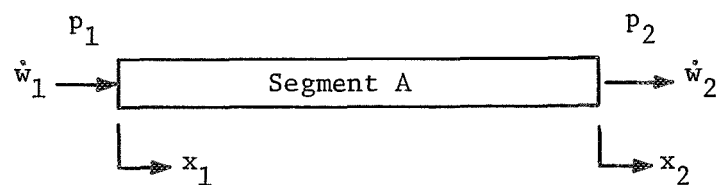
$$\ddot{x} = \sum_{i=1}^n \phi_i \ddot{q}_i$$

$$T_{O1} = T_O$$

$$T_{I1} = T_I$$

$$T_{O2} = T_O \sin \beta_E$$

$$T_{I2} = T_I \sin \beta_E$$

PROPELLANT FEEDLINE EQUATIONS

$$P_2 = P_1 - [LB]_A \dot{w}_2 - [L]_A \ddot{w}_2 - \bar{T}_{A1} \dot{x}_1 - T_{A2} \dot{x}_2 - U_{A1} \ddot{x}_1 - U_{A2} \ddot{x}_2$$

$$\dot{w}_1 = \dot{w}_{1r} - \rho A_1 \dot{x}_1$$

where

$$\bar{T}_{A1} = [\rho ALB\hat{k}]_A$$

$$\bar{T}_{A2} = [\rho ALB(1 - \hat{k})]_A$$

$$\bar{U}_{A1} = [\rho AL\hat{k}]_A$$

$$\bar{U}_{A2} = [\rho AL(1 - \hat{k})]_A$$

PUMP CAVITATION EQUATIONS

$$\dot{w}_s - \dot{w}_d = \rho \tilde{A} (NPSP) \left[\left(p_v + NPSP \right)^{\frac{-n+1}{n}} \right] + \rho (NPSP) \left[\frac{\partial}{\partial \omega} \left(\frac{1}{K} \right) \omega \right]$$

$$NPSP = p_s + \frac{1}{2\rho g A_s^2} \left[\dot{w}_s^2 + 2\dot{w}_s \circ \dot{w}_s \right]$$

ACCUMULATOR EQUATIONS

$$p_A = L_A \dot{w}_A + R_A \dot{w}_A + C_A w_A$$

$$\dot{w}_A = \dot{w}_1 - \dot{w}_2$$

PROPULSION EQUATIONSThrust Chamber

$$T = A_t \left(C_F^\circ p_C + p_C^\circ C_F + p_C C_F \right)$$

$$C_F = \frac{\partial C_F}{\partial p_C} p_C$$

$$p_C = \frac{1}{gA_t} \left(\dot{w}_C^\circ C^* + C^{*\circ} \dot{w}_C + \dot{w}_C C^* \right)$$

$$C^* = \frac{\partial C^*}{\partial \dot{w}_C} \dot{w}_C + \frac{\partial C^*}{\partial MR} MR$$

$$\dot{w}_C = \dot{w}_{CO} + \dot{w}_{CF}$$

$$MR = \frac{\dot{w}_{CO} - MR^\circ \dot{w}_{CF}}{\dot{w}_{CF}^\circ + \dot{w}_{CF}}$$

Gas Generator

$$p_g = \frac{1}{gA_{tg}} \left(\dot{w}_g^\circ C_g^* + \dot{w}_g C_g^{*\circ} + \dot{w}_g C_g^* \right)$$

$$C_g^* = \frac{\partial C_g^*}{\partial \dot{w}_g} \dot{w}_g + \frac{\partial C_g^*}{\partial MRG} MRG$$

$$\dot{w}_g = \dot{w}_{gO} + \dot{w}_{gF}$$

$$MRG = \frac{\dot{w}_{gO} - MRG^\circ \dot{w}_{gF}}{\dot{w}_{gF}^\circ + \dot{w}_{gF}}$$

Pump

$$(p_{dO} - p_{sO}) = \frac{\partial (p_{dO} - p_{sO})}{\partial p_{sO}} p_{sO} + \frac{\partial (p_{dO} - p_{sO})}{\partial \dot{w}_{dO}} \dot{w}_{dO} + \frac{\partial (p_{dO} - p_{sO})}{\partial N_{TO}} N_{TO}$$

$$(p_{dF} - p_{sF}) = \frac{\partial (p_{dF} - p_{sF})}{\partial p_{sF}} p_{sF} + \frac{\partial (p_{dF} - p_{sF})}{\partial \dot{w}_{dF}} \dot{w}_{dF} + \frac{\partial (p_{dF} - p_{sF})}{\partial N_{TF}} N_{TF}$$

$$P_{PO} = \frac{1}{\rho_O \eta_O} \left[\dot{w}_{dO}^\circ (p_{dO} - p_{sO}) + (p_{dO}^\circ - p_{sO}^\circ) \dot{w}_{dO} + \dot{w}_{dO} (p_{dO} - p_{sO}) + p_{sO} \Delta \dot{w}_O + p_{sO}^\circ \Delta \dot{w}_O \right]$$

$$\Delta \dot{w}_O = \dot{w}_{dO} - \dot{w}_{sO}$$

$$P_{PF} = \frac{1}{\rho_F \eta_F} \left[\dot{w}_{dF}^\circ (p_{dF} - p_{sF}) + (p_{dF}^\circ - p_{sF}^\circ) \dot{w}_{dF} + p_{sF}^\circ \Delta \dot{w}_F + \dot{w}_{dF} (p_{dF} - p_{sF}) + p_{sF} \Delta \dot{w}_F \right]$$

$$\Delta w_F = \dot{w}_{dF} - \dot{w}_{sF}$$

$$P_{PF} = N_{TF}^\circ M_{PF} + M_{PF}^\circ N_{TF} + N_{TF} M_{PF}$$

$$P_{PO} = N_{TO}^\circ M_{PO} + M_{PO}^\circ N_{TO} + N_{TO} M_{PO}$$

Turbine

$$P_{TF} = N_{TF}^\circ L_{TF} + L_{TF}^\circ N_{TF} + L_{TF} N_{TF}$$

$$P_{TO} = N_{TO}^\circ L_{TO} + L_{TO}^\circ N_{TO} + L_{TO} N_{TO}$$

$$I_F \dot{N}_{TF} = L_{TF} - M_{PF}$$

$$I_O \dot{N}_{TO} = L_{TO} - M_{PO}$$

Turbine (cont)

$$P_{TF} = 9336 \eta_{TF} (\dot{H}_{TIF} - \dot{H}_{TEF})$$

$$\dot{H}_{TIF} = \dot{w}_g \circ h_{TIF} + h_{TIF} \circ \dot{w}_g + \dot{w}_g h_{TIF}$$

$$h_{TIF} = C_{pTIF} T_g + \frac{\partial h_{TIF}}{\partial p_{TIF}} p_{TIF}$$

$$T_g = \frac{\partial T_g}{\partial MRG} MRG + \frac{\partial T_g}{\partial p_g} p_g$$

$$\dot{H}_{TEF} = \dot{w}_{TEF} \circ h_{TEF} + h_{TEF} \circ \dot{w}_{TEF} + h_{TEF} \dot{w}_{TEF}$$

$$h_{TEF} = C_{pTEF} T_{TEF} + \frac{\partial h_{TEF}}{\partial p_{TEF}} p_{TEF}$$

$$T_{TEF} = \left(T_g \circ + T_g \right) \left(\frac{p_{TEF} \circ + p_{TEF}}{p_{TIF} \circ + p_{TIF}} \right)^{\frac{k-1}{k}} - T_{TEF} \circ$$

$$P_{TO} = 9336 \eta_{TO} (\dot{H}_{TIO} - \dot{H}_{TEO})$$

$$\dot{H}_{TIO} = \dot{w}_{TIO} \circ h_{TIO} + h_{TIO} \circ \dot{w}_{TIO} + h_{TIO} \dot{w}_{TIO}$$

$$h_{TIO} = C_{pTIO} T_{TIO} + \frac{\partial h_{TIO}}{\partial p_{TIO}} p_{TIO}$$

$$\dot{H}_{TEO} = \dot{w}_{TEO} \circ h_{TEO} + h_{TEO} \circ \dot{w}_{TEO} + h_{TEO} \dot{w}_{TEO}$$

$$h_{TEO} = C_{pTEO} T_{TEO} + \frac{\partial h_{TEO}}{\partial p_{TEO}} p_{TEO}$$

$$T_{TEO} = \left(T_{TIO} \circ + T_{TIO} \right) \left(\frac{p_{TEO} \circ + p_{TEO}}{p_{TIO} \circ + p_{TIO}} \right)^{\frac{k-1}{k}} - T_{TEO} \circ$$

$$T_{TEF} = T_{TIO}$$

DISCHARGE EQUATIONSOxidizer Side

$$- (1 - K_{PU}) P_{dO} + (1 - K_{PU}) P_{sO} + R_{LO} \dot{w}_{LO} + I_{LO} \ddot{w}_{LO} \\ + R_{dO} \dot{w}_{dO} + I_{dO} \ddot{w}_{dO} = 0$$

$$K_{PU} P_{dO} + (1 - K_{PU}) P_{sO} - P_C + R_{LO} \dot{w}_{LO} + I_{LO} \ddot{w}_{LO} \\ - (R_{3O} + R_{2O}) \dot{w}_{COi} + (-I_{3O} - I_{2O}) \ddot{w}_{COi} \\ - R_{2O} \dot{w}_{gO} - I_{2O} \ddot{w}_{gO} = 0$$

$$P_C - P_g + R_{3O} \dot{w}_{COi} + (I_{3O}) \ddot{w}_{COi} - R_{gO} \dot{w}_{gO} \\ - I_{gO} \ddot{w}_{gO} = 0$$

$$\dot{w}_{dO} = \dot{w}_{LO} + \dot{w}_{gO} + \dot{w}_{COi}$$

$$\dot{w}_{CO} = \dot{w}_{COi} + \rho_O A_{CO} \dot{x}_{GP}$$

Fuel Side

$$P_{dF} = P_C + R_{3F} \dot{w}_{CFi} + I_{3F} \ddot{w}_{CFi} + R_{2F} \dot{w}_{dF} + I_{2F} \ddot{w}_{dF}$$

$$P_C - P_g + R_{3F} \dot{w}_{CFi} + I_{3F} \ddot{w}_{CFi} - R_{gF} \dot{w}_{gF} - I_{gF} \ddot{w}_{gF} = 0$$

$$\dot{w}_{dF} = \dot{w}_{gF} + \dot{w}_{CFi}$$

$$\dot{w}_{CF} = \dot{w}_{CFi} + \rho_F A_{CF} \dot{x}_{GP}$$

Gas Generator Loop

$$p_g = p_{TIF} + R_{gge} \dot{w}_g + I_{gge} \dot{w}_g$$

$$p_{TEF} = p_{TIO} + R_{COD} \dot{w}_g + I_{COD} \dot{w}_g$$

$$p_{TEO} = p_n + R_{OTE} \dot{w}_g + I_{OTE} \dot{w}_g$$

$$\dot{w}_g = \dot{w}_{TEF} = \dot{w}_{TIO}$$

$$p_n = \frac{p_n^{\circ}}{p_C^{\circ}} p_C$$

5.0 REFERENCES

1. Streeter, V.L., "Handbook of Fluid Dynamics", McGraw-Hill, 1961.
2. Shapiro, A. H., "The Dynamics and Thermodynamics of Compressible Fluid Flow - Vol. II", Ch. 23, Ronald Press Co., 1953.
3. Nortronics-Huntsville, Huntsville, Alabama, "An Investigation of Saturn V Coupled Longitudinal Structural Vibration and Lateral Bending Response During Boost Flight", TR-795-8-458, Dec. 1968. Prepared under Contract NAS8-20082 for NASA-Marshall Space Flight Center.
4. General Dynamics/Convair, San Diego, California, "A Study of System-Coupled Longitudinal Instabilities in Liquid Rockets, Part I - Analytic Model", AFRPL-TR-65-163, September 1965. Prepared under Contract No. AF04(611)-9956 for AF Rocket Propulsion Laboratory.
5. Martin Co., Denver, Colorado, "Dynamic Analysis of Longitudinal Oscillations of SM-68B Stage 1 (POGO)", CR-64-71 (BSD TR 65-179), March 1964. Prepared under Contract No. AF 04(647)-576 for the Ballistic Systems Division of the Air Force Systems Command.
6. Martin Marietta Corp., Baltimore, Maryland, "A Method for Determining the POGO Stability of Large Launch Vehicles", TR 69-7C, June 1969, Subcontract No. 10005 to Bellcomm, Inc.
7. The Martin Company, Denver, Colorado, "System Coupled Dynamic Instability Amplitude Limiting Analysis and Evaluation", MCR-68-20-PT-1 and MCR-68-20-PT-2, March 1968, prepared under Contract F04611-67-C-0031.
8. The Martin Company, Denver, Colorado, "A Study of System Coupled Instability Analysis Techniques, Part 1," CR-66-36-PT-1, July 1966, prepared under Contract AF04(611)-10795.
9. The Martin Company, Denver, Colorado, "A Study of System Coupled Instability Analysis Techniques, Part 2," CR-66-36-PT-2, July 1966, prepared under contract AF04(611)-10795.
10. Zucrow, M.J., "Aircraft and Missile Propulsion", Vol. II. John Wiley and Sons, 1958.